https://doi.org/10.5194/gmd-2023-203
Preprint. Discussion started: 19 January 2024

Geoscientific Model Development Discussions

E3SM Chemistry Diagnostics Package (ChemDyg) Version 0.1.4

Hsiang-He Lee*[1], Qi Tang[1], and Michael J. Prather[2]

[1]Lawrence Livermore National Laboratory, Livermore, CA, U.S.A.

[2]University of California, Irvine, CA, U.S.A.

*Corresponding author address: Dr. Hsiang-He Lee, 7000 East Avenue, Livermore, CA, 94550, U.S.A.

E-mail: lee1061@llnl.gov

https://doi.org/10.5194/gmd-2023-203
Preprint. Discussion started: 19 January 2024

Geoscientific Model Development Discussions

Abstract

The E3SM Chemistry diagnostics package (ChemDyg) is an open-source software, all diagnostic scripts written in Python, developed to support the Department of Energy (DOE) Energy Exascale Earth System Model (E3SM). The current version 0.1.4 of ChemDyg generates several diagnostic plots and tables for model-to-model and model-to-observation comparison, including 2-dimentional contour mapping plots, diurnal and annual cycle plots, time-series plots, and comprehensive processing tables. ChemDyg is executed by zppy, which is a post-processing toolchain for E3SM written in Python. The ChemDyg codebase is designed to be modular, and each diagnostics set is self-contained. Each set has its own driving script that includes set-specific file input/output and a main python script for calculation and plotting. The outputs from each diagnostics set, including figures and tables, are organized in the main HTML page to make it interactive through a browser.

This paper is a comprehensive description of E3SM ChemDyg (as of version 0.1.4) including the details of each diagnostics set and its required input data formats. This tool has enough flexibility for future ChemDyg developers to increase the addition of new observational datasets and new diagnostics sets.

https://doi.org/10.5194/gmd-2023-203
Preprint. Discussion started: 19 January 2024

Geoscientific Model Development Discussions

1 Introduction

The U.S. Department of Energy (DOE) Energy Exascale Earth System Model (E3SM) version one (E3SMv1) (Golaz et al., 2019) was first released in 2018 to feed the DOE mission needs for producing robust actionable predictions of Earth system variability and change, with an emphasis on the most critical scientific questions facing the nation and DOE (Leung et al., 2020). E3SM version two (E3SMv2) (Golaz et al., 2022) released in 2021 is based on E3SMv1 with significant improvements in existing and emerging architectures and some key climate physics. The atmosphere component of E3SMv2, E3SM Atmosphere Model (EAMv2), improved the dynamic core to solve the equations of motion in a rotating reference farm with the hydrostatic and shallow atmosphere approximations (Taylor et al., 2020). Some physics schemes have been updated in EAMv2 as well to improve computational performance. For example, the internal call order and array structure of the Cloud Layers Unified By Binormals (CLUBB) (Golaz et al., 2002; Larson, 2017) have been changed to permit contiguous memory access and also to eliminate the unrealistic pockets of supersaturation that were resolved in the microphysics scheme in EAMv1. The Zhange-McFarlane deep convection scheme (Zhang and Mcfarlane, 1995) adopted two features to improve its simulated diurnal cycle precipitation (Xie et al., 2019). The upcoming version three of E3SM (E3SMv3) has interactive chemistry which includes the prognostic linearized ozone chemistry scheme version three (Linoz v3) (Prather and Hsu, 2010; Hsu and Prather, 2010) and the University of California, Irvine (UCI) chemistry mechanism (chemUCI).

The atmospheric chemistry in EAMv1 was the Ozone model version one (O3v1) which is prescribed tropospheric ozone based on decadal monthly zonal mean latitude-pressure data from the input4MIPS Ozone dataset v1.0 (Hegglin et al., 2016) and prognostic stratospheric ozone by the linearized chemistry version two (Linoz v2) (Hsu and Prather, 2009). O3v1 calculated

https://doi.org/10.5194/gmd-2023-203
Preprint. Discussion started: 19 January 2024


Geoscientific Model Development Discussions

stratospheric ozone interactively with Linoz v2, but it can result in unrealistic ozone distribution when the simulated tropopause was higher than that of the prescribed data. The model tends to assign stratospheric ozone abundance to the tropospheric model grid boxes. In EAMv2, the O3v2 model (Tang et al., 2021) was implemented to overcome the issues in the O3v1 model and to perform a more comprehensive evaluation of the ozone simulation. O3v2 is able to interact with the tropopause changes and hence captures the naturally sharp ozone cross-tropopause gradient. Furthermore, the stratosphere-troposphere exchange (STE) flux of ozone, which is an important tropospheric ozone budget term, is available to diagnose in O3v2 due to the new method of ozone sink at the lower boundary in O3v2. In the upcoming EAMv3 release, we update the stratospheric chemistry package from Linoz v2 to Linoz v3 along with the new interactive tropospheric chemistry (chemUCI). Linoz v3 extends the Linoz v2 capabilities to include more tracers important for the E3SM goals, including prognostic ozone, methane (CH_4), nitrous oxide (N_2O), and reactive nitrogen compounds (NO_y) as well as diagnostic stratospheric water vapor. chemUCI consists of 28 advected tracers for the O_3-CH_4-HO_x-NO_x-NMVOCs chemistry in the troposphere. chemUCI originated from the University of California, Irvine (UCI) chemistry transport model (CTM)'s ASAD package (Carver et al., 1997; Wild et al., 2003).

The current model evaluation packages have comprehensive diagnostic sets to evaluate the meteorological and climatic features (e.g., temperature, precipitation, radiative effects, etc.). For example, the E3SM Diagnostics Package (E3SM Diags) is a Python-based Earth System Model evaluation tool, which was developed to support E3SM development. The core set of E3SM Diags is the seasonal and annual mean physical climate for the major variables. The plot sets cover latitude-longitude maps, maps focusing on the polar regions, Pressure-Latitude zonal mean contour plots, etc. Compared to the version two of E3SM Diags, the current version 2.7 of E3SM Diags

https://doi.org/10.5194/gmd-2023-203
Preprint. Discussion started: 19 January 2024


Geoscientific Model Development Discussions

(Zhang et al., 2022) includes some new diagnostics sets for Quasi-biennial Oscillation, El Nino-Southern Oscillation, streamflow, diurnal cycle of precipitation, analysis from ARM ground-based facilities, tropical cyclone, stratospheric column ozone (SCO) and tropospheric column ozone (TCO).

As mentioned before, O3v2 in EAMv2 has a big improvement to overcome the issue of the vertical distribution of ozone abundance, especially near the tropopause, in O3v1 because the issue can result in significant impacts on the radiation transfer in E3SM. In EAMv3, the model has fully interactive chemistry in both the troposphere and stratosphere. The ozone-only diagnostics in E3SM Diags v2.7 cannot meet the EAMv3 chemistry evaluation requirements. Thus, a systematized analysis tool for E3SM chemistry is necessary for E3SM model developers.

This paper introduces a new Python package for E3SM chemistry diagnostics: ChemDyg, which has been developed to support E3SMv3 chemistry development. The paper is a comprehensive description of ChemDyg (as of version 0.1.4) including the details of each diagnostics set. An overall description of ChemDyg, code structure, associated input data, and processing of model output are given in Section 2. The detail of each diagnostics set is shown in Section 3. A discussion of future applications and a summary are provided in Section 4.

2 The overview of ChemDyg

2.1 Code structure and workflow

ChemDyg is an open-source software, and all diagnostic scripts are written in Python. ChemDyg is executed by zppy, which is a post-processing toolchain for E3SM (https://e3sm.org/resources/tools/end-to-end-processing/zppy/). A configure run script (i.e., .cfg file) in zppy controls the tasks in ChemDyg. Users have high flexibility to specify the setting at

https://doi.org/10.5194/gmd-2023-203
Preprint. Discussion started: 19 January 2024


Geoscientific Model Development Discussions

multiple levels (i.e., for general input and output information, and different time period for each sub task) in the configure run script. Users can even select fewer specific sub tasks if necessary.

Some diagnostics sets in ChemDyg request reformatted E3SM outputs (e.g., remapping, seasonal/annual mean climatology, etc.), instead of default monthly data with a native grid. The post-processing E3SM output can also be handled by zppy for running netCDF operators (http://research.jisao.washington.edu/data_sets/nco/) (see Section 2.3 for details). Observations and reanalysis data used in some diagnostics sets of ChemDyg are pre-processed, and the reference path is default assigned corresponding to different DOE machines. Figure 1 depicts a schematic overview of the code structure and workflow.

The ChemDyg codebase is designed to be modular, and each diagnostics set is self-contained. Each set has its own driving script that includes set-specific file input/output and a main Python script for calculation and plotting. The outputs from each diagnostic set, including figures and tables, are organized in the main HTML page to make it interactive through a browser.

2.2 Data involved for comparison

2.2.1 Observations of surface ozone

Analyzed 10 years (2000-2009) hourly surface ozone (O_3) data from air quality networks in North America (NA; 25-49°N and 125-67°W) and Europe (EU; 36-71°N and 11°W-34°E) is adopted from Schnell et al. (2015). The data sets used for NA are mainly from three networks: the United States (US) Environmental Protection Agency's (EPA) Air Quality System (1633 stations; http://www.epa.gov/ttn/airs/aqsdatamart), the US EPA's Clean Air Status and Trends Network (92 stations; http://epa.gov/castnet/javaweb/index.html), and Environment Canada's National Air Pollution Surveillance Program (207 stations; http://maps-cartes.ec.gc.ca/rnspa-naps/data.aspx?lang=en). The observational data sets in Europe (EU) are provided by the

https://doi.org/10.5194/gmd-2023-203
Preprint. Discussion started: 19 January 2024


Geoscientific Model Development Discussions

European Environment Agency's air quality database (2123 stations; http://www.eea.europa.eu/data-and-maps/data/) and the European Monitoring and Evaluation Programme (162 stations; Hjellbrekke et al. (2013)).

In order to have a commensurate comparison between station measurements and model simulations, the surface observed O_3 is interpolated onto the 1° × 1° hourly grid-cell averaged O_3 data over NA and EU by using the interpolation scheme described in Schnell et al. (2014). The maximum daily 8-hour averages (MDA8) are interpolated from the hourly measurements and subsequently derive the MDA8 at each grid cell (Schnell et al., 2015).

2.2.2 Surface ozone from ACCMIP and UCI CTM

The eight models in the Atmospheric Chemistry and Climate Model Intercomparison Project (ACCMIP; Lamarque et al. (2013)) with archived hourly surface O_3 are used for surface O_3 comparison in ChemDyg. The analyzed data in the plots are adopted from Schnell et al. (2015). Most ACCMIP models provide 10 years of data, starting in either model year 2000 or 2001, to closely align with observations. Table 1 provides a summary and references of the models used in this comparison. Besides the ACCMIP models, Schnell et al. (2015) also used one hindcast simulation over the same period as the observations from the University of California Irvine Chemical Transport Model (UCI CTM) (Holmes et al., 2013).

For an appropriate comparison between the models and measurements, the modeled hourly O_3 abundances (mostly at 2° to 3° resolution; Table 1) are regridded to the same 1° × 1° cells as the observations using first-order conservative mapping.

https://doi.org/10.5194/gmd-2023-203
Preprint. Discussion started: 19 January 2024


Geoscientific Model Development Discussions

149 2.2.3 Tropospheric ozone from CMIP6

150 The 3-dimensional O_3 from the five models in Phase 6 of the Coupled Model
151 Intercomparison Project (CMIP6) Historical experiments are used in ChemDyg for tropospheric
152 column ozone (TCO) comparison. We use the archived O_3 data from AERmon (CMIP6 table for
153 monthly atmospheric chemistry and aerosol data) to derive the tropospheric O_3 burden on the
154 model grids, along with the tropopause using the World Meteorological Organization (WMO)
155 definition of tropopause on 3-dimension temperature. The selected models are based on Griffiths
156 et al. (2021). The O_3 data are available for from 1850 to 2014, and a short summary of CMIP6
157 models is presented in Table 2.

158 2.2.4 Observations for ozone hole evaluation

159 The observational metrics used for O_3 hole evaluation are daily geographically resolved
160 total column ozone (TOZ), which are collected from three satellite remote sensing data: the Total
161 Ozone Mapping Spectrometer (TMOS) on the NASA/NOAA Nimbus-7 satellite (Mcpeters et al.,
162 1996), the Ozone Monitoring Instrument (OMI) on the Aura satellite (Schoeberl et al., 2004), and
163 the Ozone Mapper and Profiler Suite (OMPS) on NASA's Suomi National Polar-orbiting
164 Partnership (NPP) satellite (Flynn et al., 2014). Based on these daily TOZ data, the NASA Ozone
165 Watch website (https://ozonewatch.gsfc.nasa.gov) compiles the daily records of the Antarctic
166 ozone hole area defined as TOZ < 220 DU (Dobson units, milli-cm-amagats) and minimum TOZ
167 in the Southern Hemisphere (SH). The data obtained from the Ozone Watch website are used in
168 ChemDyg to evaluate model simulations.

https://doi.org/10.5194/gmd-2023-203
Preprint. Discussion started: 19 January 2024

169 #### 2.2.5 NOAA surface carbon monoxide

170 The observed surface carbon monoxide (CO) is from the Global Greenhouse Gas
171 Reference Network for the Carbon Cycle and Greenhouse Gases (CCGG) Group, which is part of
172 NOAA's Global Monitoring Laboratory (GML) in Boulder, Colorado (Petron et al., 2022). The
173 Reference Network measures four greenhouse gases which are the main long-term drivers of
174 climate change and important indicators of air pollution: carbon dioxide (CO_2), methane (CH_4),
175 nitrous oxide (N_2O), and CO. The Reference Network measurement program collects data mainly
176 from in-situ measurements at four baseline background sites and 8 tall towers. Besides long-term
177 in-situ observations, flask-air samples are collected by volunteers at over 50 additional regional
178 background sites and from small aircraft. The observed CO metrics used in ChemDyg are flask-
179 air samples (see
180 https://gml.noaa.gov/aftp/data/trace_gases/co/flask/surface/README_surface_flask_co.html for
181 details) collected from 12 stations (Table 3) for model evaluation, and the observational data cover
182 the period from 1988 to 2021.

183 ### 2.3 Pre-processing of model output

184 Due to the purpose of each chemistry diagnostics set, besides the default monthly mean
185 E3SM output (h0 files), three types of time frequency output are required for ChemDyg: monthly
186 (0 in `nhtfrq`) instantaneous ('I' in `avgflag_pertape`) output (for example, h1 files), hourly (-1
187 in `nhtfrq`) instantaneous output (for example, h2 files), and daily (-24 in `nhtfrq`) averaged ('A'
188 in `avgflag_pertape`) output (for example, h3 files). Appendix A shows an example setup of
189 E3SM run script to generate these three types of time frequency output in the coordinated output
190 files (h1~h3) with the associated variables. Note that `history_gaschmbudget_num` should be the

https://doi.org/10.5194/gmd-2023-203
Preprint. Discussion started: 19 January 2024


Geoscientific Model Development Discussions

same as the monthly instantaneous output (here is h1 in Appendix A). The E3SM filenames can be changed according to user preference and specified in the ChemDyg run script.

The pre-processing tasks include generating regridded climatology from the monthly output, and regridded monthly/hourly time-series files, as input for various diagnostics sets in ChemDyg. The default format of E3SM output is on a native grid. In order to have a commensurate comparison to observations or for the plotting purpose, the model outputs need to regrid to different resolutions. The most common one is to interrelate to a 1° × 1° grid as the CMIP6 format. As we mentioned in Section 2.2.2, the metrics for surface O_3 comparison are required to be remapped to the same 1° × 1° cells as the observations but covering the selected area in NA and EU only.

3 Examples of diagnostics

Version 0.1.4 of ChemDyg generates 11 types of plots and four types of tables for model-to-model and model-to-observation comparison, including 2-dimensional contour mapping plots, diurnal and annual cycle plots, time-series plots, and comprehensive processing tables. Table 4 shows a summary of the basic sets of diagnostics in ChemDyg, including a short description, supported model input format (i.e., native/regarded grid and time-series/climatology), and associated observations/reanalysis data. This section shows some examples to illustrate the application of this diagnostics package in evaluating E3SM chemistry. Note that all diagnostics figures/tables included in this paper were extracted from several ChemDyg runs which are simulated from E3SMv3 testbase candidates for demonstration purposes.

https://doi.org/10.5194/gmd-2023-203
Preprint. Discussion started: 19 January 2024


Geoscientific Model Development Discussions

3.1 Pressure-Latitude plots

Ozone abundance and distribution is one of the main focuses of E3SMv3 chemistry development. This diagnostics set includes Pressure-Latitude zonal mean contour plots of annual mean O_3, O_3 in troposphere only (O_3 Trop), specific humidity (Q), and temperature (T). These figures provide the overall of O_3 vertical profile associated with potential temperature gradient and other related parameters (i.e., Q and T). Figure 2 demonstrates a Pressure-Latitude plot of multi-year zonal mean O_3 abundance and potential temperature. We also present the zonal mean O_3 profile for the standard E3SMv2 simulation and their differences to evaluate the O_3 implementation in E3SMv3.

E3SMv2 uses the World Meteorological Organization (WMO) defined tropopause, which is the lowest level at which the temperature lapse rate decreases to 2 K per km or less, with the average lapse rate between this level and all higher levels within 2 km. Based on this definition, the model is hard to illustrate a folded tropopause due to a frontal system or other 3-dimensional (3D) tropopause structure. Thus, in E3SMv3 chemistry, we introduce an artificial tracer called E90 to define a tropopause that effectively separates stratospheric air from tropospheric air from a chemical composition perspective (Prather et al., 2011). This diagnostics set also shows the WMO defined tropopause (the yellow line in Fig. 2a and the cyan line in Fig. 2b)) and E90 defined 3D tropopause (the magenta line in Fig. 2a) side by side.

3.2 Latitude-Longitude plots

Meteorological factors affect the chemical processes and alter chemistry concentrations, including O_3. In a recent study (Sitnov et al., 2017), precipitable water vapor and total column O_3 have strong connections with the North Atlantic Oscillation. Thus, we highlight total precipitable water (TMQ) (Fig. 3) in ChemDyg.

https://doi.org/10.5194/gmd-2023-203
Preprint. Discussion started: 19 January 2024


Geoscientific Model Development Discussions

3.3 Nitrogen oxides (NO_x) emission plots

Nitrogen oxides (NO_x) emissions have been a constant concern because of their role in air pollution leading to smog and acidic wet and dry deposition. NO_x are also important in affecting global O_3 concentrations through their chemical reactions with hydrocarbons and then as O_3 precursors. The largest sources of NO_x in the troposphere are fossil fuel combustion, biomass burning, lightning discharges, aircraft emissions, and microbial activity in soils through biogeochemistry processes. This diagnostics set mainly focuses on lighting discharges and aircraft emissions (Fig. 4).

3.4 Tropospheric column ozone (TCO) comparison

Ozone is a short-lived reactive gas and an oxidizing species with adverse effects on human health (Lippmann, 1991). Tropospheric O_3 production is from the photochemical oxidation of CO, CH_4, and non-methane volatile organic compounds (NMVOCs) in the presence of nitrogen oxides (i.e., NO and NO_2). Thus, the TCO burden is controlled by the balance between chemical production and loss processes (Section 3.11). The O_3 production and loss vary between models due to different approaches in representing the processes involved and different budget terms defined. The definition of tropopause also affects the diagnosed TCO burden and any influx from the stratosphere. Based on Griffiths et al. (2021), we examine TCO for five CMIP6 models (Table 2) which are derived from the archived O_3 and tropopause data from AERmon. This diagnostics set is designed to compare the time series of global mean TCO between E3SM and the CMIP6 models (Fig. 5).

3.5 Surface ozone diurnal and annual cycle comparison

Following the method in Schnell et al. (2015) using air quality networks to evaluate modeled surface O_3, 10 years (2000-2009) hourly surface O_3 measurements from air quality

https://doi.org/10.5194/gmd-2023-203
Preprint. Discussion started: 19 January 2024


Geoscientific Model Development Discussions

networks in NA and EU and the ACCMIP model simulated surface O_3 (Table 1) are used in this diagnostics set to evaluate E3SM surface O_3 performance. Because of different chemistry regions, the analysis domain in NA is split into western (WNA) and eastern (ENA) regions at 96°W, and in EU is split into southern (SEU) and northern (NEU) regions at 53°N.

The diagnostics set of surface O_3 diurnal provides diurnal cycles of hourly O_3 abundance averaged over winter (DJF) shown in Fig. 6a and summer (JJA). The set of annual cycles is particularly for MDA8 O_3 abundance (Fig. 6b).

3.6 Surface CO comparison

As we mentioned in Section 3.1, TCO production is from the photochemical oxidation of CO and other chemical species. CO is one of the main precursors of O_3 production. Compared to O_3, the lifetime of CO is longer, about two months, to make CO a good indicator for regional air quality. This diagnostics set uses NOAA surface CO collected from 12 stations (Table 3) for E3SM model evaluation. Figure 7 shows the time series of surface CO burden from observation (red solid line) and E3SM (black solid line) at the BRW observational site. We also calculate the mean, anomaly, and tendency of surface CO burden during the analyzed period.

3.7 Ozone hole

Antarctic ozone hole commonly is defined by three types of metrics: the area of the hole (adding the areas below the same threshold in the total column ozone (TOZ) field), the minimum TOZ value within the hole, and the Antarctic ozone mass deficit (Uchino et al., 1999; Huck et al., 2007). Since 1990, the evolution of the Antarctic ozone hole has been driven primarily by dynamical variation due to the chlorine levels driving ozone depletion inside the Antarctic winter vortex. Several previous studies have calculated indicators of Antarctic ozone depletion and

https://doi.org/10.5194/gmd-2023-203
Preprint. Discussion started: 19 January 2024


Geoscientific Model Development Discussions

Uchino et al. (1999) examined the changes in the area of the Antarctic ozone hole using a threshold of TOZ less than 220 DU and the ozone mass deficiency within the ozone hole.

In this diagnostics set, we use the daily ozone hole diagnostics from the NASA Ozone Watch website as a reference and two metrics: the area with less than 220 DU in TOZ and the minimum TOZ (Fig. 8) to evaluate the model capability for capturing the ozone hole variation compared to the observations.

3.8 Total column ozone and temperature with equivalent latitude

Bodeker et al. (2002) used the satellite data to analyze the long-term evolution of the Antarctic ozone hole and its dependence on the size of the dynamical vortex and meridional temperature structure within the polar vortex because the 2000 ozone hole was the largest on record. In their study, the vortex has strengthened from 1981 to 2000, and the average equivalent latitude location of the center of the vortex edge has remained unchanged at ~62°S over the 20 years. Here, equivalent latitude zonal means of these data have been calculated to show the expansion of the Antarctic ozone hole and its encroachment on the vortex edge. Furthermore, they calculated daily equivalent latitude zonal mean 550 K temperature isentrope profiles and found from Jun to August the equivalent latitude at which the temperature profiles fall below 195 K has changed little over the 20-year period. Thus, the increase in the size of the Antarctic ozone hole during the period was not caused by either the increase in the size of the dynamical vortex or the area of temperatures below 195 K.

The diagnostics set of TOZ with equivalent latitude has similar methods as Bodeker et al. (2002) to analyze daily TOZ with equivalent latitude at 64°S to provide time series and daily evolution of the minimum TOZ with equivalent latitude (64°S) area from 1 July to 31 December as measured by the minimum total column ozone (Fig. 9).

https://doi.org/10.5194/gmd-2023-203
Preprint. Discussion started: 19 January 2024


Geoscientific Model Development Discussions

The diagnostics set of temperature with equivalent latitude is to calculate the mean temperature averaged from 1 July to 31 December at three different altitudes (i.e., 14, 20, and 25 km) with various equivalent latitudes from 60°S to 78°S (Figure 10). It can help us to indicate the approximate temperature for polar stratospheric cloud formation (it was set as 197.5 K in E3SMv2 but now is 198 K in E3SMv3). Because this diagnostics set is computationally expensive, we suggest users only turn on this set when it is necessary.

3.9 Ozone stratosphere-troposphere exchange flux

The stratosphere-troposphere exchange (STE) flux of ozone is a key budget term for tropospheric ozone abundance. As mentioned before, in O3v2 the net STE ozone flux is estimated from the loss in the near surface atmospheric layers (lowest four layers). This approach can limit the global mean ozone flux based on proxy relationships with other trace gases, giving us a broad range of 400-600 Tg O_3 per year (Murphy and Fahey, 1994; Mclinden et al., 2000; Olsen et al., 2004; Olsen et al., 2001; Hsu et al., 2005). Ozone is conserved in the rest of the troposphere and thus the STE flux is taken up by these lowest layers. It is resolved geographically and monthly but because of the tropospheric transport from the tropopause to the lowest layers, the STE ozone flux diagnosed this way will differ from the tropopause-crossing flux in location and with a slight time delay of less than a month (Jacob, 1999). Figure 11 shows thee time series and mean annual cycle in the north hemisphere (NH), south hemisphere (SH), and global.

3.10 Chemistry tendency table

The diagnostics set of chemistry tendency is designed to help E3SM model developers pinpoint the simulation errors from potential chemistry processes when the model generates unrealistic chemistry abundance. The tendency calculation is driven by the chemistry driver in E3SM chemistry module from 10 processes: implicit solver (TDI), explicit solver (TDE), aerosol-

https://doi.org/10.5194/gmd-2023-203
Preprint. Discussion started: 19 January 2024


Geoscientific Model Development Discussions

gas exchange (TDA), chemistry processes from Linoz (TDL), reset negative values (TDN), setting upper boundary values (TDU), setting lower boundary values (TDB), surface emission (TDS), dry deposition (TDD), and wet deposition (WD). Chemistry tendency outside the chemistry module (e.g., dynamic driven transport) is considered in TDO. The tendency is due to the reset mixing ratio in the stratosphere after the implicit solver and explicit solver are characterized as TRI and TRE, respectively. Figure 12 shows a schematic workflow of chemistry tendency processes and their associated working files.

Those tendency outputs are a column integrated 2-dimentional format for each chemistry tracer to minimize the file size. In order to better understand the chemistry processes crossing different vertical layers in the atmosphere, we classify the entire model column into 4 layers based on the standard 72 model layers: top of the model to 100 hPa (L1), 100 to 267 hPa (L2), 267 to 856 hPa (L3), and 856 hPa to the surface (L4). Variables associated with the Linoz process (i.e., variables named O3, N2OLNZ, and CH4LNZ) have a specific output layer for the troposphere (trop). Users can decide how to classify these 4 layers in the E3SM run script as shown in Appendix A. This diagnostics set generates annual and seasonal chemistry tendency tables with both HTML and text formats.

3.11 Chemistry closure check and burden table

The diagnostics set is designed for the closure check of each chemical species by calculating Level-2 normalization relative difference between the sum of total tendencies listed in Fig. 12 and the difference of chemistry burden (MSD) before and after the tendency calculated. A table generated by this diagnostics set lists not only the chemistry closure check but also the mean concentration (Tg) and volume mixing ratio (mol mol^{-1}) of each chemical species estimated after dry deposition.

https://doi.org/10.5194/gmd-2023-203
Preprint. Discussion started: 19 January 2024


Geoscientific Model Development Discussions

Note that the diagnostics set of the chemistry tendency table mentioned in Section 3.10 requires annual mean climatology data, while the diagnostics set of chemistry closure check needs monthly time-series output. Thus, this diagnostics set requests more computational resources, and the diagnostics period should be enough for one or two years.

3.12 Chemistry production and loss tendency table

This diagnostic table focuses on the O_3 production and loss in the implicit solver and the CO production and loss in the explicit solver.

The tropospheric O_3 abundance is dominated by the balance between chemical production and loss processes, deposition at the surface, and downward transport from the stratosphere. In order to check the O_3 production and loss tendency in the implicit solver, we calculate each chemical reaction for O_3 production and loss used in chemUCI (Appendix B) and then sum of reactions for the production (TIP) and loss (TIL) tendency right after the implicit solver. After the implicit solver, the chemistry module is to reset the volume mixing ratio in the stratosphere to the mixing ratio before the implicit solver for all chemical species because the stratospheric chemistry is handled by Linoz v3. The chemistry module also resets the diagnostic reaction rate in the stratosphere to zero. The tendency due to the stratospheric volume mixing ratio reset after the implicit solver is identified as TRI in the tendency table. After the stratospheric volume mixing ratio reset, we calculate the sum of chemical reactions for the O_3 production (CIP) and loss (CIL) again for a final chemistry closure check after the implicit solver and the stratospheric volume mixing ratio reset. Figure 13 shows a schematic workflow of chemistry tendency processes for the O_3 production and loss diagnostics in the implicit solver and after the stratospheric reset.

Current chemical reactions for the O_3 production and loss used in chemUCI (Appendix B) miss some important reactions with NO and NO_2. We also calculate the chemistry reactions

https://doi.org/10.5194/gmd-2023-203
Preprint. Discussion started: 19 January 2024


Geoscientific Model Development Discussions

suggested by Prof. Michael Prather (see in Appendix B) for the O_3 production and loss (MPP and MPL) in the tendency diagnostic table for comparison.

The mixing ratio tendency of CO is handled by the explicit solver (TDE). The production (TEP) and loss (TEL) tendency are calculated in one subroutine (i.e., `exp_prod_loss`) and the code structure is relatively straightforward compared to the implicit solver. The tendency due to the stratospheric volume mixing ratio reset after the explicit solver is set as TRE in the tendency table. After the stratospheric diagnostic reaction reset (important in the explicit solver), we call the subroutine again to calculate the CO production (CEP) and loss (CEL) tendency for a final chemistry closure check after the explicit solver and the stratospheric volume mixing ratio reset.

3.13 Chemistry high-level summary table

The chemistry high-level summary table provides a short summary for O_3, CO, and NO_x. The summary table for O_3 includes burden, deposition, production, loss, net change from production and loss, TCO, SCO, and STE. Those are introduced in other diagnostics sets in the previous sections. The summary table for CO includes burden, emission, deposition, production, loss, and net change from production and loss. Regarding NO_x, the summary table shows their total burden, emission, and deposition. Once NOx emission variables from lighting (NO_TDLgt) and aircraft (NO2_TDAcf) are available in the E3SM outputs, they will be presented in the summary table as well.

4 Discussion and summery

This paper introduces a new Python package for E3SM chemistry diagnostic - ChemDyg, which is developed to support E3SMv3 chemistry development. The chemistry tendency table is generated from the diagnostics set designed for E3SM developers to identify the chemistry processes for unrealistic chemistry abundance. Because the diagnostics set uses the annual and

https://doi.org/10.5194/gmd-2023-203
Preprint. Discussion started: 19 January 2024


Geoscientific Model Development Discussions

seasonal mean climatology input data, it is easy to overlook the errors from the time step or diurnal scale. Thus, we provide one stand-alone Python script, called `DEBUG_chem_diags_timestep.py` (`https://github.com/E3SM-Project/ChemDyg/blob/main/DEBUG_chem_diags_timestep.py`) to generate a chemistry tendency table for each time step, hourly or daily basis depends on the time frequency of output file.

A completed ChemDyg diagnostics requires extra chemistry outputs compared to other E3SM diagnostics packages. In order to reduce the maximum number of E3SM outputs but keep essential variables for ChemDyg, we designed a simplified version of ChemDyg to remove the outputs for the chemistry tendency table and the chemistry closure check table (roughly reducing 70% of full diagnostics outputs). The users only need to turn on the flag of `history_chemdyg_summary` in the E3SM run script and turn off other diagnostic flags (i.e., `history_gaschmbudget_2D`, `history_gaschmbudget_2D_levels`, `history_UCIgaschmbudget_2D`, and `history_UCIgaschmbudget_2D_levels` in Appendix A).

The current released version (v0.1.4) of ChemDyg generates 11 types of plots and 4 types of tables for model-to-model and model-to-observation comparison (Table 4), mainly for E3SM chemistry. The diagnostic package includes 2-dimentional contour mapping plots, diurnal and annual cycle plots, time-series plots, and comprehensive processing tables. The upcoming version 0.1.5 of ChemDyg will not only generate plots but also their corresponding data in the NetCDF format. The users only need to turn on the flag, ncfile_save = 'true', in the .cfg run script. ChemDyg will continue to develop as one of the main evaluation packages for component models of E3SM, focusing on more chemistry species in future development.

Regarding technical enhancements, some diagnostics sets request more nodes and longer computational time, especially for the table of chemistry closure check and the plot of temperature

https://doi.org/10.5194/gmd-2023-203
Preprint. Discussion started: 19 January 2024

with equivalent latitudes. Further improvement is needed to solve I/O and computational limitations of zeep (walltime and the number of nodes).

Appendix A: E3SM output requirement

This section provides an example setup to generate necessary variables for ChemDyg when running E3SM on DOE supercomputers. Note that the paths of input data might change on different supercomputers.

```
cat << EOF >> user_nl_eam

nhtfrq = 0,0,-1,-24
mfilt = 1,1,240,30

avgflag_pertape = 'A','I','I','A'
history_gaschmbudget_num = 2
fincl1='E90','N2OLNZ','NOYLNZ','H2OLNZ','CH4LNZ', 'TOZ',
‘O3’,’OH’,’HO2’,’H2O2’,’NO’,’NO2’,’NO3’,’N2O5’,’HNO3’,’HO2NO2’,’CO’,’CH2O’,’C
H3O2’,’CH3OOH’,’DMS’,’SO2’,’ISOP’,’H2SO4’,’SOAG’,’C2H5OOH’,’CH3CHO’,'PS',
'lch4','r_lch4',
 fincl3 = 'O3_SRF'

 tropopause_e90_thrd            = 80.0e-9

 history_chemdyg_summary = .false.
 history_gaschmbudget = .false.
 history_gaschmbudget_2D = .true.
 history_gaschmbudget_2D_levels = .true.
 history_UCIgaschmbudget_2D = .true.
 history_UCIgaschmbudget_2D_levels = .true.
 gaschmbudget_2D_L1_s =  1
 gaschmbudget_2D_L1_e = 26
 gaschmbudget_2D_L2_s = 27
 gaschmbudget_2D_L2_e = 38
 gaschmbudget_2D_L3_s = 39
 gaschmbudget_2D_L3_e = 58
 gaschmbudget_2D_L4_s = 59
 gaschmbudget_2D_L4_e = 72

 linoz_psc_t = 198.0

 …
```

https://doi.org/10.5194/gmd-2023-203
Preprint. Discussion started: 19 January 2024

Geoscientific Model Development Discussions

```
EOF
```

Appendix B: Chemistry reactions for ozone production and loss

The following chemical reaction and loss processes are based on E3SMv3.
The chemical reaction for ozone production in chemUCI (TIP/CIP):

```
NO2 + hv -> NO + O3
NO3 + hv -> NO2 + O3
N2O5 + hv -> NO + O3 + NO3
OH + OH -> O3 + H2O
```

The chemical reaction for ozone loss in chemUCI (TIL/CIL):

```
O3 + H2O -> 2*OH
O3 + H2 -> OH + HO2
O3 + CH4LNZ -> OH + {CH3OO}
C2H4 + O3 -> CH2O + CO + 0.5*CH3CHO
ISOP + O3 -> MVKMACR + CH2O + OH
OH + O3 -> HO2 + O2
HO2 + O3 -> 2*O2 + OH
NO + O3 -> NO2 + O2
NO2 + O3 -> NO3 + O2
MVKMACR + O3 -> 0.5*CH3CO3 + CH2O + CH3O2
Heterogeneous reaction
```

The chemical reaction for ozone production suggested by Prof. Michael Prather (MPP):

```
CH3O2 + NO -> CH2O + HO2 + NO2
NO + HO2 -> NO2 + OH
C2H5O2 + NO -> CH3CHO + HO2 + NO2
CH3CO3 + NO -> CH3O2 + NO2
ROHO2 + NO -> CH3CHO + CH2O + NO2
ISOPO2 + NO -> MVKMACR + CH2O + NO2
MVKO2 + NO -> 0.5*CH3CO3 + CH2O + NO2
```

The chemical reaction for ozone loss suggested by Prof. Michael Prather (MPL):

```
O3 + H2O -> 2*OH
O3 + H2 -> OH + HO2
O3 + CH4LNZ -> OH + {CH3OO}
C2H4 + O3 -> CH2O + CO + 0.5*CH3CHO
ISOP + O3 -> MVKMACR + CH2O + OH
OH + O3 -> HO2 + O2
HO2 + O3 -> 2*O2 + OH
MVKMACR + O3 -> 0.5*CH3CO3 + CH2O + CH3O2
```

Code and data availability:

https://doi.org/10.5194/gmd-2023-203
Preprint. Discussion started: 19 January 2024


Geoscientific Model Development Discussions

The ChemDyg code (v0.1.4) used in this study has been released on Zenodo (https://doi.org/10.5281/zenodo.10116320). The observational data used in ChemDyg are available at https://doi.org/10.5281/zenodo.8274422. Other E3SMv3 simulated outputs for the plots in this paper are available at https://doi.org/10.5281/zenodo.8415473.

Sample availability:

This link provides an example of a complete ChemDyg run with a testing version of E3SMv3 output https://web.lcrc.anl.gov/public/e3sm/diagnostic_output/ac.lee1061/20220914.PAN.MZThet.v2.LR.bi-grid.amip.chemUCI_Linozv3/e3sm_chem_diags/plots/. Other information of ChemDyg can be found on https://e3sm.org/resources/tools/diagnostic-tools/chemdyg/.

Author contributions:

H.-H. Lee and all coauthors provided ideas and designed the diagnostics sets in ChemDyg. H.-H. Lee and Q. Tang contributed to code and data development to ChemDyg. H.-H. Lee leads and coordinates the manuscript with input from coauthors.

Competing interests.

The contact author has declared that none of the authors has any competing interests.

Acknowledgements:

https://doi.org/10.5194/gmd-2023-203
Preprint. Discussion started: 19 January 2024

This work is supported by the Energy Exascale Earth System Model (E3SM) project funded by the U.S. Department of Energy, Office of Science, Office of Biological and Environmental Research. Part of the study supported by the LLNL LDRD project 22-ERD-008, "Multiscale Wildfire Simulation Framework and Remote Sensing". Work at LLNL was performed under the auspices of the U.S. DOE by Lawrence Livermore National Laboratory under contract DE-AC52-07NA27344. LLNL IM: LLNL-JRNL-855846-DRAFT.

Reference:

Archibald, A. T., O'Connor, F. M., Abraham, N. L., Archer-Nicholls, S., Chipperfield, M. P., Dalvi, M., Folberth, G. A., Dennison, F., Dhomse, S. S., Griffiths, P. T., Hardacre, C., Hewitt, A. J., Hill, R. S., Johnson, C. E., Keeble, J., Köhler, M. O., Morgenstern, O., Mulcahy, J. P., Ordóñez, C., Pope, R. J., Rumbold, S. T., Russo, M. R., Savage, N. H., Sellar, A., Stringer, M., Turnock, S. T., Wild, O., and Zeng, G.: Description and evaluation of the UKCA stratosphere–troposphere chemistry scheme (StratTrop vn 1.0) implemented in UKESM1, Geosci. Model Dev., 13, 1223-1266, 10.5194/gmd-13-1223-2020, 2020.

Bauer, S. E., Tsigaridis, K., Faluvegi, G., Kelley, M., Lo, K. K., Miller, R. L., Nazarenko, L., Schmidt, G. A., and Wu, J.: Historical (1850–2014) Aerosol Evolution and Role on Climate Forcing Using the GISS ModelE2.1 Contribution to CMIP6, Journal of Advances in Modeling Earth Systems, 12, e2019MS001978, https://doi.org/10.1029/2019MS001978, 2020.

Bodeker, G. E., Struthers, H., and Connor, B. J.: Dynamical containment of Antarctic ozone depletion, Geophysical Research Letters, 29, 2-1-2-4, https://doi.org/10.1029/2001GL014206, 2002.

Cameron-Smith, P., Lamarque, J. F., Connell, P., Chuang, C., and Vitt, F.: Toward an Earth system model: atmospheric chemistry, coupling, and petascale computing, Journal of Physics: Conference Series, 46, 343-350, 10.1088/1742-6596/46/1/048, 2006.

Carver, G. D., Brown, P. D., and Wild, O.: The ASAD atmospheric chemistry integration package and chemical reaction database, Computer Physics Communications, 105, 197-215, https://doi.org/10.1016/S0010-4655(97)00056-8, 1997.

Deushi, M. and Shibata, K.: Development of a Meteorological Research Institute Chemistry-Climate Model version 2 for the Study of Tropospheric and Stratospheric Chemistry, Papers in Meteorology and Geophysics, 62, 1-46, 10.2467/mripapers.62.1, 2011.

Donner, L. J., Wyman, B. L., Hemler, R. S., Horowitz, L. W., Ming, Y., Zhao, M., Golaz, J.-C., Ginoux, P., Lin, S.-J., Schwarzkopf, M. D., Austin, J., Alaka, G., Cooke, W. F., Delworth, T. L., Freidenreich, S. M., Gordon, C. T., Griffies, S. M., Held, I. M., Hurlin, W. J., Klein, S. A., Knutson, T. R., Langenhorst, A. R., Lee, H.-C., Lin, Y., Magi, B. I., Malyshev, S. L., Milly, P. C. D., Naik, V., Nath, M. J., Pincus, R., Ploshay, J. J., Ramaswamy, V., Seman, C. J., Shevliakova, E., Sirutis, J. J., Stern, W. F., Stouffer, R. J., Wilson, R. J., Winton, M., Wittenberg, A. T., and Zeng, F.: The Dynamical Core, Physical Parameterizations, and Basic Simulation

https://doi.org/10.5194/gmd-2023-203
Preprint. Discussion started: 19 January 2024

559 Characteristics of the Atmospheric Component AM3 of the GFDL Global Coupled Model CM3,
560 Journal of Climate, 24, 3484-3519, 10.1175/2011jcli3955.1, 2011.
561 Dunne, J. P., Horowitz, L. W., Adcroft, A. J., Ginoux, P., Held, I. M., John, J. G., Krasting, J. P.,
562 Malyshev, S., Naik, V., Paulot, F., Shevliakova, E., Stock, C. A., Zadeh, N., Balaji, V., Blanton,
563 C., Dunne, K. A., Dupuis, C., Durachta, J., Dussin, R., Gauthier, P. P. G., Griffies, S. M., Guo,
564 H., Hallberg, R. W., Harrison, M., He, J., Hurlin, W., McHugh, C., Menzel, R., Milly, P. C. D.,
565 Nikonov, S., Paynter, D. J., Ploshay, J., Radhakrishnan, A., Rand, K., Reichl, B. G., Robinson,
566 T., Schwarzkopf, D. M., Sentman, L. T., Underwood, S., Vahlenkamp, H., Winton, M.,
567 Wittenberg, A. T., Wyman, B., Zeng, Y., and Zhao, M.: The GFDL Earth System Model Version
568 4.1 (GFDL-ESM 4.1): Overall Coupled Model Description and Simulation Characteristics,
569 Journal of Advances in Modeling Earth Systems, 12, e2019MS002015,
570 https://doi.org/10.1029/2019MS002015, 2020.
571 Emmons, L. K., Schwantes, R. H., Orlando, J. J., Tyndall, G., Kinnison, D., Lamarque, J.-F.,
572 Marsh, D., Mills, M. J., Tilmes, S., Bardeen, C., Buchholz, R. R., Conley, A., Gettelman, A.,
573 Garcia, R., Simpson, I., Blake, D. R., Meinardi, S., and Pétron, G.: The Chemistry Mechanism in
574 the Community Earth System Model Version 2 (CESM2), Journal of Advances in Modeling
575 Earth Systems, 12, e2019MS001882, https://doi.org/10.1029/2019MS001882, 2020.
576 Flynn, L., Long, C., Wu, X., Evans, R., Beck, C. T., Petropavlovskikh, I., McConville, G., Yu,
577 W., Zhang, Z., Niu, J., Beach, E., Hao, Y., Pan, C., Sen, B., Novicki, M., Zhou, S., and Seftor,
578 C.: Performance of the Ozone Mapping and Profiler Suite (OMPS) products, Journal of
579 Geophysical Research: Atmospheres, 119, 6181-6195, https://doi.org/10.1002/2013JD020467,
580 2014.
581 Gettelman, A., Hannay, C., Bacmeister, J. T., Neale, R. B., Pendergrass, A. G., Danabasoglu, G.,
582 Lamarque, J.-F., Fasullo, J. T., Bailey, D. A., Lawrence, D. M., and Mills, M. J.: High Climate
583 Sensitivity in the Community Earth System Model Version 2 (CESM2), Geophysical Research
584 Letters, 46, 8329-8337, https://doi.org/10.1029/2019GL083978, 2019.
585 Golaz, A. J.-C., Roekel, L. P. V., Zheng, X., Roberts, A., Wolfe, J. D., Lin, W., Bradley, A.,
586 Tang, Q., Maltrud, M. E., ., R. M. F., and et al.: The DOE E3SM Model Version 2: Overview of
587 the physical model and initial model evaluation, Earth and Space Science Open Archive, 68,
588 doi:10.1002/essoar.10511174.2,
589 Golaz, J.-C., Larson, V. E., and Cotton, W. R.: A PDF-Based Model for Boundary Layer Clouds.
590 Part I: Method and Model Description, Journal of the Atmospheric Sciences, 59, 3540-3551,
591 10.1175/1520-0469(2002)059<3540:APBMFB>2.0.CO;2, 2002.
592 Golaz, J.-C., Van Roekel, L. P., Zheng, X., Roberts, A. F., Wolfe, J. D., Lin, W., Bradley, A. M.,
593 Tang, Q., Maltrud, M. E., Forsyth, R. M., Zhang, C., Zhou, T., Zhang, K., Zender, C. S., Wu, M.,
594 Wang, H., Turner, A. K., Singh, B., Richter, J. H., Qin, Y., Petersen, M. R., Mametjanov, A.,
595 Ma, P.-L., Larson, V. E., Krishna, J., Keen, N. D., Jeffery, N., Hunke, E. C., Hannah, W. M.,
596 Guba, O., Griffin, B. M., Feng, Y., Engwirda, D., Di Vittorio, A. V., Dang, C., Conlon, L. M.,
597 Chen, C.-C.-J., Brunke, M. A., Bisht, G., Benedict, J. J., Asay-Davis, X. S., Zhang, Y., Zhang,
598 M., Zeng, X., Xie, S., Wolfram, P. J., Vo, T., Veneziani, M., Tesfa, T. K., Sreepathi, S., Salinger,
599 A. G., Reeves Eyre, J. E. J., Prather, M. J., Mahajan, S., Li, Q., Jones, P. W., Jacob, R. L.,
600 Huebler, G. W., Huang, X., Hillman, B. R., Harrop, B. E., Foucar, J. G., Fang, Y., Comeau, D.
601 S., Caldwell, P. M., Bartoletti, T., Balaguru, K., Taylor, M. A., McCoy, R. B., Leung, L. R., and
602 Bader, D. C.: The DOE E3SM Model Version 2: Overview of the Physical Model and Initial
603 Model Evaluation, Journal of Advances in Modeling Earth Systems, 14, e2022MS003156,
604 https://doi.org/10.1029/2022MS003156, 2022.

https://doi.org/10.5194/gmd-2023-203
Preprint. Discussion started: 19 January 2024

Geoscientific Model Development Discussions

605 Golaz, J.-C., Caldwell, P. M., Van Roekel, L. P., Petersen, M. R., Tang, Q., Wolfe, J. D.,
606 Abeshu, G., Anantharaj, V., Asay-Davis, X. S., Bader, D. C., Baldwin, S. A., Bisht, G.,
607 Bogenschutz, P. A., Branstetter, M., Brunke, M. A., Brus, S. R., Burrows, S. M., Cameron-
608 Smith, P. J., Donahue, A. S., Deakin, M., Easter, R. C., Evans, K. J., Feng, Y., Flanner, M.,
609 Foucar, J. G., Fyke, J. G., Griffin, B. M., Hannay, C., Harrop, B. E., Hoffman, M. J., Hunke, E.
610 C., Jacob, R. L., Jacobsen, D. W., Jeffery, N., Jones, P. W., Keen, N. D., Klein, S. A., Larson, V.
611 E., Leung, L. R., Li, H.-Y., Lin, W., Lipscomb, W. H., Ma, P.-L., Mahajan, S., Maltrud, M. E.,
612 Mametjanov, A., McClean, J. L., McCoy, R. B., Neale, R. B., Price, S. F., Qian, Y., Rasch, P. J.,
613 Reeves Eyre, J. E. J., Riley, W. J., Ringler, T. D., Roberts, A. F., Roesler, E. L., Salinger, A. G.,
614 Shaheen, Z., Shi, X., Singh, B., Tang, J., Taylor, M. A., Thornton, P. E., Turner, A. K.,
615 Veneziani, M., Wan, H., Wang, H., Wang, S., Williams, D. N., Wolfram, P. J., Worley, P. H.,
616 Xie, S., Yang, Y., Yoon, J.-H., Zelinka, M. D., Zender, C. S., Zeng, X., Zhang, C., Zhang, K.,
617 Zhang, Y., Zheng, X., Zhou, T., and Zhu, Q.: The DOE E3SM Coupled Model Version 1:
618 Overview and Evaluation at Standard Resolution, Journal of Advances in Modeling Earth
619 Systems, 11, 2089-2129, 10.1029/2018ms001603, 2019.
620 Griffiths, P. T., Murray, L. T., Zeng, G., Shin, Y. M., Abraham, N. L., Archibald, A. T., Deushi,
621 M., Emmons, L. K., Galbally, I. E., Hassler, B., Horowitz, L. W., Keeble, J., Liu, J., Moeini, O.,
622 Naik, V., O'Connor, F. M., Oshima, N., Tarasick, D., Tilmes, S., Turnock, S. T., Wild, O.,
623 Young, P. J., and Zanis, P.: Tropospheric ozone in CMIP6 simulations, Atmos. Chem. Phys., 21,
624 4187-4218, 10.5194/acp-21-4187-2021, 2021.
625 Hegglin, M., Kinnison, D., Lamarque, J.-F., and Plummer, D.: CCMI ozone in support of CMIP6
626 - version 1.0, Earth System Grid Federation [dataset], 10.22033/ESGF/input4MIPs.1115, 2016.
627 Hjellbrekke, A.-G., Solberg, S., and Fjæraa, A. M.: Ozone measurements 2011, Norwegian
628 institute for Air Research, Norway, EMEP/CCC-Report 3/2013, Tech. Rep., 2013.
629 Holmes, C. D., Prather, M. J., Søvde, O. A., and Myhre, G.: Future methane, hydroxyl, and their
630 uncertainties: key climate and emission parameters for future predictions, Atmos. Chem. Phys.,
631 13, 285-302, 10.5194/acp-13-285-2013, 2013.
632 Horowitz, L. W., Naik, V., Paulot, F., Ginoux, P. A., Dunne, J. P., Mao, J., Schnell, J., Chen, X.,
633 He, J., John, J. G., Lin, M., Lin, P., Malyshev, S., Paynter, D., Shevliakova, E., and Zhao, M.:
634 The GFDL Global Atmospheric Chemistry-Climate Model AM4.1: Model Description and
635 Simulation Characteristics, Journal of Advances in Modeling Earth Systems, 12,
636 e2019MS002032, https://doi.org/10.1029/2019MS002032, 2020.
637 Hsu, J. and Prather, M. J.: Stratospheric variability and tropospheric ozone, Journal of
638 Geophysical Research: Atmospheres, 114, https://doi.org/10.1029/2008JD010942, 2009.
639 Hsu, J. and Prather, M. J.: Global long-lived chemical modes excited in a 3-D chemistry
640 transport model: Stratospheric N2O, NOy, O3 and CH4 chemistry, Geophysical Research
641 Letters, 37, https://doi.org/10.1029/2009GL042243, 2010.
642 Hsu, J., Prather, M. J., and Wild, O.: Diagnosing the stratosphere-to-troposphere flux of ozone in
643 a chemistry transport model, Journal of Geophysical Research: Atmospheres, 110,
644 https://doi.org/10.1029/2005JD006045, 2005.
645 Huck, P. E., Tilmes, S., Bodeker, G. E., Randel, W. J., McDonald, A. J., and Nakajima, H.: An
646 improved measure of ozone depletion in the Antarctic stratosphere, Journal of Geophysical
647 Research, 112, 2007.
648 Jacob, D. J.: Introduction to atmospheric chemistry, Princeton University Press1999.

https://doi.org/10.5194/gmd-2023-203
Preprint. Discussion started: 19 January 2024

Geoscientific Model Development Discussions

649 Josse, B., Simon, P., and Peuch, V. H.: Radon global simulations with the multiscale chemistry
650 and transport model MOCAGE, Tellus B: Chemical and Physical Meteorology, 56, 339-356,
651 10.3402/tellusb.v56i4.16448, 2004.
652 Koch, D., Schmidt, G. A., and Field, C. V.: Sulfur, sea salt, and radionuclide aerosols in GISS
653 ModelE, Journal of Geophysical Research: Atmospheres, 111,
654 https://doi.org/10.1029/2004JD005550, 2006.
655 Lamarque, J. F., Dentener, F., McConnell, J., Ro, C. U., Shaw, M., Vet, R., Bergmann, D.,
656 Cameron-Smith, P., Dalsoren, S., Doherty, R., Faluvegi, G., Ghan, S. J., Josse, B., Lee, Y. H.,
657 MacKenzie, I. A., Plummer, D., Shindell, D. T., Skeie, R. B., Stevenson, D. S., Strode, S., Zeng,
658 G., Curran, M., Dahl-Jensen, D., Das, S., Fritzsche, D., and Nolan, M.: Multi-model mean
659 nitrogen and sulfur deposition from the Atmospheric Chemistry and Climate Model
660 Intercomparison Project (ACCMIP): evaluation of historical and projected future changes,
661 Atmos. Chem. Phys., 13, 7997-8018, 10.5194/acp-13-7997-2013, 2013.
662 Larson, V. E.: CLUBB-SILHS: A parameterization of subgrid variability in the atmosphere,
663 arXiv preprint arXiv:1711.03675, 2017.
664 Leung, L. R., Bader, D. C., Taylor, M. A., and McCoy, R. B.: An Introduction to the E3SM
665 Special Collection: Goals, Science Drivers, Development, and Analysis, Journal of Advances in
666 Modeling Earth Systems, 12, e2019MS001821, https://doi.org/10.1029/2019MS001821, 2020.
667 Lippmann, M.: Health effects of tropospheric ozone, Environmental science & technology, 25,
668 1954-1962, 1991.
669 McLinden, C. A., Olsen, S. C., Hannegan, B., Wild, O., Prather, M. J., and Sundet, J.:
670 Stratospheric ozone in 3-D models: A simple chemistry and the cross-tropopause flux, Journal of
671 Geophysical Research: Atmospheres, 105, 14653-14665, https://doi.org/10.1029/2000JD900124,
672 2000.
673 McPeters, R. D., Bhartia, P. K., Krueger, A. J., and Herman, J. R.: Nimbus-7 total ozone
674 mapping spectrometer (TOMS) data products user's guide, National Aeronautics and Space
675 Administration, Scientific and Technical Information Branch1996.
676 Mulcahy, J. P., Johnson, C., Jones, C. G., Povey, A. C., Scott, C. E., Sellar, A., Turnock, S. T.,
677 Woodhouse, M. T., Abraham, N. L., Andrews, M. B., Bellouin, N., Browse, J., Carslaw, K. S.,
678 Dalvi, M., Folberth, G. A., Glover, M., Grosvenor, D. P., Hardacre, C., Hill, R., Johnson, B.,
679 Jones, A., Kipling, Z., Mann, G., Mollard, J., O'Connor, F. M., Palmiéri, J., Reddington, C.,
680 Rumbold, S. T., Richardson, M., Schutgens, N. A. J., Stier, P., Stringer, M., Tang, Y., Walton, J.,
681 Woodward, S., and Yool, A.: Description and evaluation of aerosol in UKESM1 and HadGEM3-
682 GC3.1 CMIP6 historical simulations, Geosci. Model Dev., 13, 6383-6423, 10.5194/gmd-13-
683 6383-2020, 2020.
684 Murphy, D. M. and Fahey, D. W.: An estimate of the flux of stratospheric reactive nitrogen and
685 ozone into the troposphere, Journal of Geophysical Research: Atmospheres, 99, 5325-5332,
686 https://doi.org/10.1029/93JD03558, 1994.
687 Naik, V., Horowitz, L. W., Fiore, A. M., Ginoux, P., Mao, J., Aghedo, A. M., and Levy II, H.:
688 Impact of preindustrial to present-day changes in short-lived pollutant emissions on atmospheric
689 composition and climate forcing, Journal of Geophysical Research: Atmospheres, 118, 8086-
690 8110, https://doi.org/10.1002/jgrd.50608, 2013.
691 Olsen, M. A., Schoeberl, M. R., and Douglass, A. R.: Stratosphere-troposphere exchange of mass
692 and ozone, Journal of Geophysical Research: Atmospheres, 109,
693 https://doi.org/10.1029/2004JD005186, 2004.

https://doi.org/10.5194/gmd-2023-203
Preprint. Discussion started: 19 January 2024

694 Olsen, S. C., McLinden, C. A., and Prather, M. J.: Stratospheric N2O–NO y system: Testing
695 uncertainties in a three-dimensional framework, Journal of Geophysical Research: Atmospheres,
696 106, 28771-28784, https://doi.org/10.1029/2001JD000559, 2001.
697 Oman, L. D., Ziemke, J. R., Douglass, A. R., Waugh, D. W., Lang, C., Rodriguez, J. M., and
698 Nielsen, J. E.: The response of tropical tropospheric ozone to ENSO, Geophysical Research
699 Letters, 38, https://doi.org/10.1029/2011GL047865, 2011.
700 Petron, G., Crotwell, A. M., Crotwell, M. J., Dlugokencky, E. J., Madronich, M., Moglia, E.,
701 Neff, D., Thoning, K. W., Wolter, S., and Mund, J. W.: Atmospheric Carbon Monoxide Dry Air
702 Mole Fractions from the NOAA GML Carbon Cycle Cooperative Global Air Sampling Network,
703 1988-2021, 2022.
704 Prather, M. J. and Hsu, J.: Coupling of Nitrous Oxide and Methane by Global Atmospheric
705 Chemistry, Science, 330, 952-954, doi:10.1126/science.1196285, 2010.
706 Prather, M. J., Zhu, X., Tang, Q., Hsu, J., and Neu, J. L.: An atmospheric chemist in search of
707 the tropopause, J. Geophys. Res., 116, D04306, 10.1029/2010jd014939, 2011.
708 Schnell, J. L., Holmes, C. D., Jangam, A., and Prather, M. J.: Skill in forecasting extreme ozone
709 pollution episodes with a global atmospheric chemistry model, Atmos. Chem. Phys., 14, 7721-
710 7739, 10.5194/acp-14-7721-2014, 2014.
711 Schnell, J. L., Prather, M. J., Josse, B., Naik, V., Horowitz, L. W., Cameron-Smith, P.,
712 Bergmann, D., Zeng, G., Plummer, D. A., Sudo, K., Nagashima, T., Shindell, D. T., Faluvegi,
713 G., and Strode, S. A.: Use of North American and European air quality networks to evaluate
714 global chemistry–climate modeling of surface ozone, Atmos. Chem. Phys., 15, 10581-10596,
715 10.5194/acp-15-10581-2015, 2015.
716 Schoeberl, M. R., Douglass, A. R., Hilsenrath, E., Bhartia, P. K., Barnett, J., Gille, J., Beer, R.,
717 Gunson, M., Waters, J., Levelt, P. F., and DeCola, P.: Earth Observing System missions benefit
718 atmospheric research, Eos, Transactions American Geophysical Union, 85, 177-181,
719 https://doi.org/10.1029/2004EO180001, 2004.
720 Scinocca, J. F., McFarlane, N. A., Lazare, M., Li, J., and Plummer, D.: Technical Note: The
721 CCCma third generation AGCM and its extension into the middle atmosphere, Atmos. Chem.
722 Phys., 8, 7055-7074, 10.5194/acp-8-7055-2008, 2008.
723 Shindell, D. T., Pechony, O., Voulgarakis, A., Faluvegi, G., Nazarenko, L., Lamarque, J. F.,
724 Bowman, K., Milly, G., Kovari, B., Ruedy, R., and Schmidt, G. A.: Interactive ozone and
725 methane chemistry in GISS-E2 historical and future climate simulations, Atmos. Chem. Phys.,
726 13, 2653-2689, 10.5194/acp-13-2653-2013, 2013.
727 Sitnov, S. A., Mokhov, I. I., and Bezverkhny, V. A.: Connections of Precipitable Water Vapor
728 and Total Ozone Anomalies over European Russia with the North Atlantic Oscillation: Specific
729 Features of Summer 2010, Izvestiya, Atmospheric and Oceanic Physics, 53, 885-893,
730 10.1134/S0001433817090286, 2017.
731 Tang, Q., Prather, M. J., Hsu, J., Ruiz, D. J., Cameron-Smith, P. J., Xie, S., and Golaz, J. C.:
732 Evaluation of the interactive stratospheric ozone (O3v2) module in the E3SM version 1 Earth
733 system model, Geosci. Model Dev., 14, 1219-1236, 10.5194/gmd-14-1219-2021, 2021.
734 Taylor, M. A., Guba, O., Steyer, A., Ullrich, P. A., Hall, D. M., and Eldred, C.: An Energy
735 Consistent Discretization of the Nonhydrostatic Equations in Primitive Variables, Journal of
736 Advances in Modeling Earth Systems, 12, e2019MS001783,
737 https://doi.org/10.1029/2019MS001783, 2020.
738 Teyssèdre, H., Michou, M., Clark, H. L., Josse, B., Karcher, F., Olivié, D., Peuch, V. H., Saint-
739 Martin, D., Cariolle, D., Attié, J. L., Nédélec, P., Ricaud, P., Thouret, V., van der A, R. J., Volz-

https://doi.org/10.5194/gmd-2023-203
Preprint. Discussion started: 19 January 2024

740 Thomas, A., and Chéroux, F.: A new tropospheric and stratospheric Chemistry and Transport
741 Model MOCAGE-Climat for multi-year studies: evaluation of the present-day climatology and
742 sensitivity to surface processes, Atmos. Chem. Phys., 7, 5815-5860, 10.5194/acp-7-5815-2007,
743 2007.
744 Tilmes, S., Hodzic, A., Emmons, L. K., Mills, M. J., Gettelman, A., Kinnison, D. E., Park, M.,
745 Lamarque, J.-F., Vitt, F., Shrivastava, M., Campuzano-Jost, P., Jimenez, J. L., and Liu, X.:
746 Climate Forcing and Trends of Organic Aerosols in the Community Earth System Model
747 (CESM2), Journal of Advances in Modeling Earth Systems, 11, 4323-4351,
748 https://doi.org/10.1029/2019MS001827, 2019.
749 Uchino, O., Bojkov, R. D., Balis, D. S., Akagi, K., Hayashi, M., and Kajihara, R.: Essential
750 characteristics of the Antarctic-Spring Ozone Decline: Update to 1998, Geophysical Research
751 Letters, 26, 1377-1380, https://doi.org/10.1029/1999GL900277, 1999.
752 Watanabe, S., Hajima, T., Sudo, K., Nagashima, T., Takemura, T., Okajima, H., Nozawa, T.,
753 Kawase, H., Abe, M., Yokohata, T., Ise, T., Sato, H., Kato, E., Takata, K., Emori, S., and
754 Kawamiya, M.: MIROC-ESM 2010: model description and basic results of CMIP5-20c3m
755 experiments, Geosci. Model Dev., 4, 845-872, 10.5194/gmd-4-845-2011, 2011.
756 Wild, O., Sundet, J. K., Prather, M. J., Isaksen, I. S. A., Akimoto, H., Browell, E. V., and
757 Oltmans, S. J.: Chemical transport model ozone simulations for spring 2001 over the western
758 Pacific: Comparisons with TRACE-P lidar, ozonesondes, and Total Ozone Mapping
759 Spectrometer columns, Journal of Geophysical Research: Atmospheres, 108,
760 https://doi.org/10.1029/2002JD003283, 2003.
761 Xie, S., Wang, Y.-C., Lin, W., Ma, H.-Y., Tang, Q., Tang, S., Zheng, X., Golaz, J.-C., Zhang, G.
762 J., and Zhang, M.: Improved Diurnal Cycle of Precipitation in E3SM With a Revised Convective
763 Triggering Function, Journal of Advances in Modeling Earth Systems, 11, 2290-2310,
764 https://doi.org/10.1029/2019MS001702, 2019.
765 Yukimoto, S., Kawai, H., Koshiro, T., Oshima, N., Yoshida, K., Urakawa, S., Tsujino, H.,
766 Deushi, M., Tanaka, T., Hosaka, M., Yabu, S., Yoshimura, H., Shindo, E., Mizuta, R., Obata, A.,
767 Adachi, Y., and Ishii, M.: The Meteorological Research Institute Earth System Model Version
768 2.0, MRI-ESM2.0: Description and Basic Evaluation of the Physical Component, Journal of the
769 Meteorological Society of Japan. Ser. II, 97, 931-965, 10.2151/jmsj.2019-051, 2019.
770 Zeng, G., Pyle, J. A., and Young, P. J.: Impact of climate change on tropospheric ozone and its
771 global budgets, Atmos. Chem. Phys., 8, 369-387, 10.5194/acp-8-369-2008, 2008.
772 Zeng, G., Morgenstern, O., Braesicke, P., and Pyle, J. A.: Impact of stratospheric ozone recovery
773 on tropospheric ozone and its budget, Geophysical Research Letters, 37,
774 https://doi.org/10.1029/2010GL042812, 2010.
775 Zhang, C., Golaz, J. C., Forsyth, R., Vo, T., Xie, S., Shaheen, Z., Potter, G. L., Asay-Davis, X.
776 S., Zender, C. S., Lin, W., Chen, C. C., Terai, C. R., Mahajan, S., Zhou, T., Balaguru, K., Tang,
777 Q., Tao, C., Zhang, Y., Emmenegger, T., Burrows, S., and Ullrich, P. A.: The E3SM Diagnostics
778 Package (E3SM Diags v2.7): a Python-based diagnostics package for Earth system model
779 evaluation, Geosci. Model Dev., 15, 9031-9056, 10.5194/gmd-15-9031-2022, 2022.
780 Zhang, G. J. and McFarlane, N. A.: Sensitivity of climate simulations to the parameterization of
781 cumulus convection in the Canadian climate centre general circulation model, Atmosphere-
782 Ocean, 33, 407-446, 10.1080/07055900.1995.9649539, 1995.
783
784
785

https://doi.org/10.5194/gmd-2023-203
Preprint. Discussion started: 19 January 2024

Geoscientific Model Development Discussions
Open Access
EGU

Table 1. A summary of the ACCMIP models and UCI CTM for the surface O_3 comparison

Model	Member*	Resolution (lat. × lon.)	Number of years	References
MOCAGE	r2i1p1	2° × 2°	4	Josse et al. (2004) Teyssèdre et al. (2007)
GFDL-AF3	r1i1p1	2° × 2.5°	10	Donner et al. (2011) Naik et al. (2013)
CESM-CAM-SF	r1i1p1	~1.9° × 2.5°	10	Cameron-Smith et al. (2006) Lamarque et al. (2013)
UM-CAM	r1i1p1	2.5° × 3.75°	10	Zeng et al. (2008) Zeng et al. (2010)
CMAM	r1i1p1	~3.7° × 3.75°	10	Scinocca et al. (2008)
MIROC-CHEM	r1i1p1	~2.8° × 2.8125°	10	Watanabe et al. (2011)
GISS-E2-R	r1i1p3	2° × 2.5°	5	Koch et al. (2006) Shindell et al. (2013)
GEOSCCM	r1i1p1	2° × 2.5°	10	Oman et al. (2011)
UCI CTM	-	~2.8° × 2.8125°	10	Holmes et al. (2013)

* The format *r* <*N*> *i* <*M*> *p* <*L*> defines each model simulation's realization number (N), initialization method (M), and perturbed physics version (L).

https://doi.org/10.5194/gmd-2023-203
Preprint. Discussion started: 19 January 2024

Geoscientific Model Development Discussions

790 Table 2. A summary of the CMIP6 models the tropospheric O_3 comparison

Model	Member*	Resolution (lat. × lon.)	Vertical layers	References
CESM2-WACCM	r1i1p1	0.9° × 1.25°	70	(Gettelman et al., 2019) (Tilmes et al., 2019) (Emmons et al., 2020)
GFDL-ESM4	r1i1p1	1° × 1.25°	49	(Horowitz et al., 2020) (Dunne et al., 2020)
GISS-E2-1-G	r1i1p3	2° × 2.5°	40	(Bauer et al., 2020)
MRI-ESM2-0	r1i1p1	2.813° × 2.813°	80	(Deushi and Shibata, 2011) (Yukimoto et al., 2019)
UKESM1-0-LL	r1i1p1	1.25° × 1.875°	85	(Archibald et al., 2020) (Mulcahy et al., 2020)

791 * The format *r <N> i <M> p <L>* defines each model simulation's realization number (N), initialization method
792 (M), and perturbed physics version (L).
793

https://doi.org/10.5194/gmd-2023-203
Preprint. Discussion started: 19 January 2024

Geoscientific Model Development Discussions

794 Table 3. A summary of NOAA surface CO observational sites

Code	Name	Country	Latitude	Longitude	Elevation (meters)
BRW	Barrow Atmospheric Baseline Observatory	United States	71.323	-156.611	11.0
CGO	Cape Grim, Tasmania	Australia	-40.683	144.690	94.0
ICE	Storhofdi, Vestmannaeyjar	Iceland	63.400	-20.288	118.0
KUM	Cape Kumukahi, Hawaii	United States	19.561	-154.888	8.0
MHD	Mace Head, County Galway	Ireland	53.326	-9.899	5.0
MID	Sand Island, Midway	United States	28.219	-177.368	4.6
PSA	Palmer Station, Antarctica	United States	-64.774	-64.053	10.0
RPB	Ragged Point	Barbados	13.165	-59.432	15.0
SMO	Tutuila	American Samoa	-14.247	-170.564	42.0
SYO	Syowa Station, Antarctica	Japan	-69.013	39.590	14.0
WIS	Weizmann Institute of Science at the Arava Institute, Ketura	Israel	29.965	35.060	151.0
ZEP	Ny-Alesund, Svalbard	Norway and Sweden	78.907	11.888	474.0

795
796
797
798

https://doi.org/10.5194/gmd-2023-203
Preprint. Discussion started: 19 January 2024

Geoscientific Model Development Discussions

799 Table 4. A summary of the basic set of diagnostics in ChemDyg

Set of plots/tables	Description	Supported model input format	Associated observations/reanalysis data (with year range and data format)
Pressure-Latitude plots	Pressure-Latitude zonal mean contour plots of annual mean ozone (O_3), ozone in troposphere only (O_3 Trop), specific humidity (Q), and temperature (T)	Annual mean regridded (180×360) climatology	Standard E3SMv2 results (Golaz et al.) (1985-2014)
Latitude-Longitude plots	Latitude-Longitude contour map of annual mean vertically intergraded total precipitable water (TMQ)	Annual mean regridded (180×360) climatology	N/A
NO_x emission plots	The vertical profile and Latitude-Longitude contour map of annual mean NO_x emissions from aircraft and lightning	Annual mean regridded (180×360) climatology	N/A
TCO comparison	Time series global mean Tropospheric ozone (TCO) burden	Monthly regridded (180×360) time-series	CMIP6 (References see Table 2) (1985-2014)
Surface ozone diurnal cycle comparison	Seasonal mean hour plot of global mean surface ozone	Hourly regridded (1.0×1.0) time-series	CMIP6 (Schnell et al., 2015) (2000-2009)
Surface ozone annual cycle comparison	Annual mean month plot of global mean surface ozone	Hourly regridded (1.0×1.0) time - series	CMIP6 (Schnell et al., 2015) (2000-2009)
Surface CO comparison	Time series plot and anomalies of surface CO at NOAA ground-based facilities	Monthly regridded (180×360) time-series	NOAA surface stations (Petron et al., 2022) (1990-2020)
Ozone hole	Annal mean day plot of ozone hole area and minimum ozone burden in the south hemisphere	Daily time-series	Observations (https://ozonewatch.gsfc.nasa.gov/SH.html) (1990-2019)
Ozone hole with equivalent latitude	Time series plot and annual mean month plot of total column ozone burden with equivalent latitude	Daily time-series	N/A
Ozone STE flux	Time series plot and annual mean month plot of ozone stratosphere-	Monthly time-series	N/A

https://doi.org/10.5194/gmd-2023-203
Preprint. Discussion started: 19 January 2024

Geoscientific Model Development Discussions

	troposphere-exchange (STE) flux		
Temperature with equivalent latitude	Seasonal mean Latitude plot of temperature at specific layer with equivalent latitude	Daily time-series	N/A
Chemistry tendency table	Seasonal and annual mean chemistry tendency metrics summarized in tables	Annual mean climatology	N/A
Chemistry closure check and burden	Annual mean chemistry metrics and L2-normalization relative difference in a table	Monthly time-series	N/A
Chemistry production/loss tendency table	Seasonal and annual mean O_3 and CO production and loss tendency metrics summarized in tables	Annual mean climatology	N/A
Chemistry high-level summary table	Annual mean O_3, CO, and CH_4 metrics summarized in a table	Monthly time-series	N/A

800
801

https://doi.org/10.5194/gmd-2023-203
Preprint. Discussion started: 19 January 2024

Geoscientific Model Development Discussions

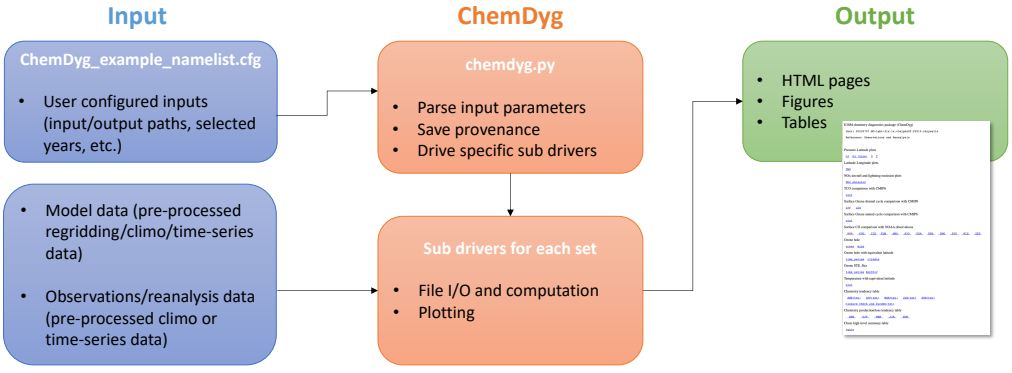

Figure 1. A schematic overview of ChemDyg structure and workflow. The primary input (blue boxes) includes the user configuration through setting up a python configure script (i.e., the .cfg file), model data pre-processed from native E3SM history files, and reformatted observation/reanalysis data. The run scripts for model data pre-processing are also controlled by the configure script. The main ChemDyg (orange boxes) parses the user input and drives individual sub-drivers for specified diagnostics set. The output (green box) includes a HTML page linking to each individual figures and tables.

https://doi.org/10.5194/gmd-2023-203
Preprint. Discussion started: 19 January 2024

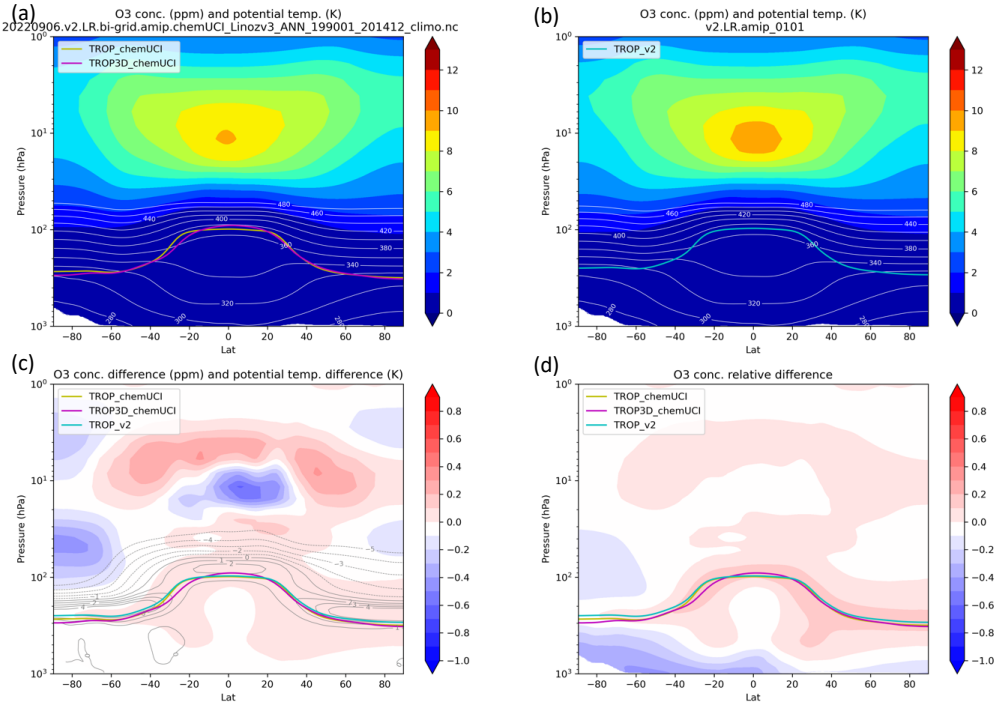

Figure 2. (a) Pressure-Latitude plot of multi-year zonal mean ozone abundance (contours; units: ppm) and potential temperature (white lines; units: K) from a E3SMv3 testing simulation. Yellow line and magenta line show the WMO defined tropopause and 3D tropopause, respectively. (b) is same as (a) but for the standard E3SMv2 simulation. Cyan line shows the WMO defined tropopause. (c) and (d) are the absolute difference and the relative difference of (a) and (b), respectively.

https://doi.org/10.5194/gmd-2023-203
Preprint. Discussion started: 19 January 2024

Geoscientific Model Development Discussions
Open Access
EGU

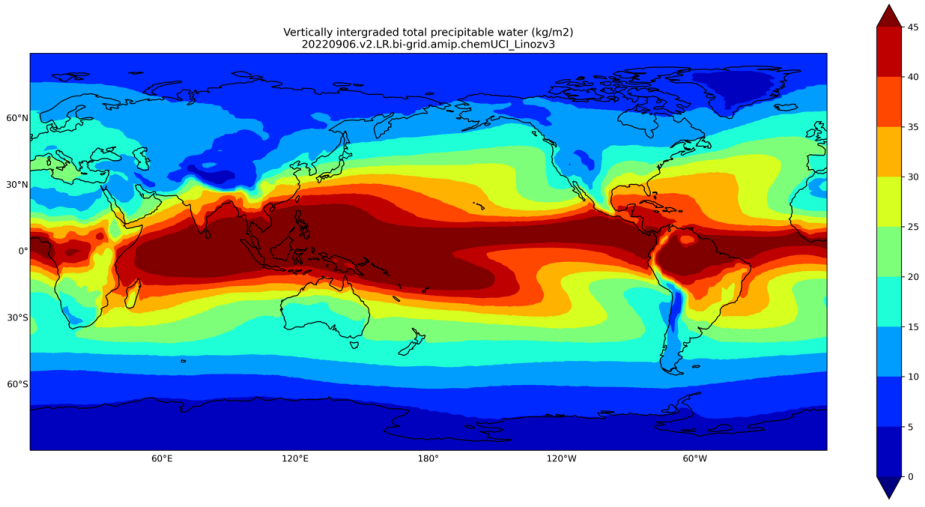

Figure 3. Latitude-Longitude contour map of annual mean vertically intergraded total precipitable water (TMQ; units: kg/m^2) from a E3SMv3 testing simulation.

https://doi.org/10.5194/gmd-2023-203
Preprint. Discussion started: 19 January 2024

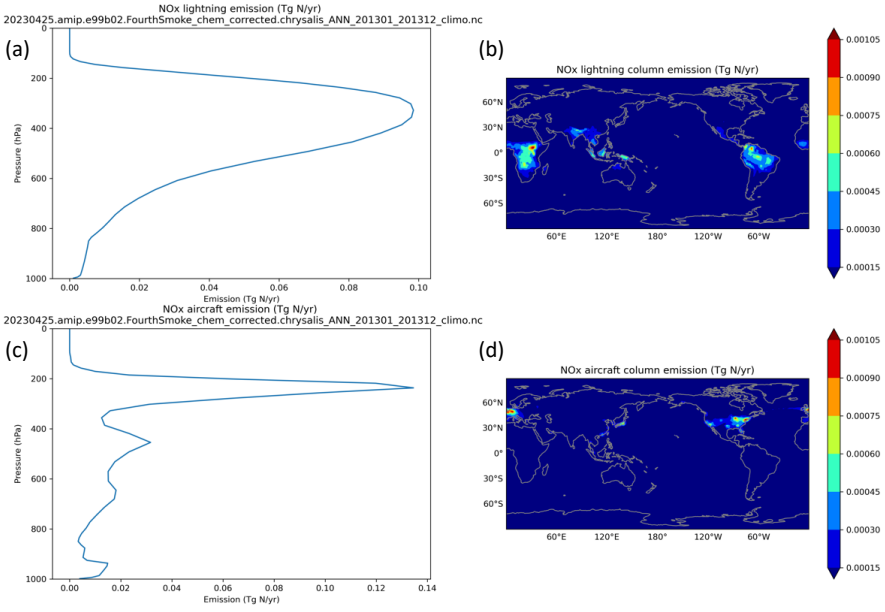

Figure 4. (a) The vertical profile of global sum lightning discharged NO_x (units: Tg N/year) and (b) Latitude-Longitude contour map of annual mean vertically intergraded lighting NO_x (units: Tg N/year) from a E3SMv3 testing simulation. (c) and (d) are the same as (a) and (b) but for aircraft emitted NO_x.

https://doi.org/10.5194/gmd-2023-203
Preprint. Discussion started: 19 January 2024

Geoscientific Model Development Discussions
Open Access
EGU

832

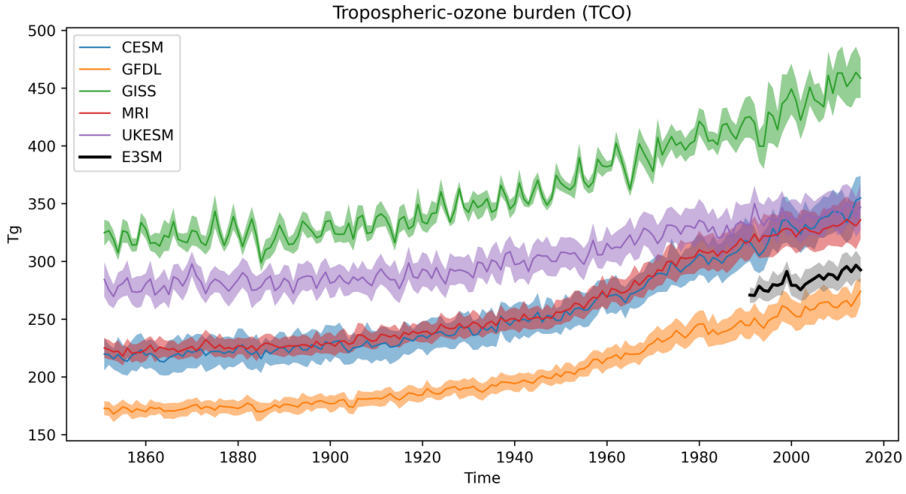

833
834 Figure 5. Time series of global mean tropospheric column ozone (TCO) burden (units: Tg) in 5
835 CMIP6 models listed on Table 2 and E3SM (black line). The shading shows the mean ± 1
836 standard deviation of the monthly variability for each year.
837

https://doi.org/10.5194/gmd-2023-203
Preprint. Discussion started: 19 January 2024

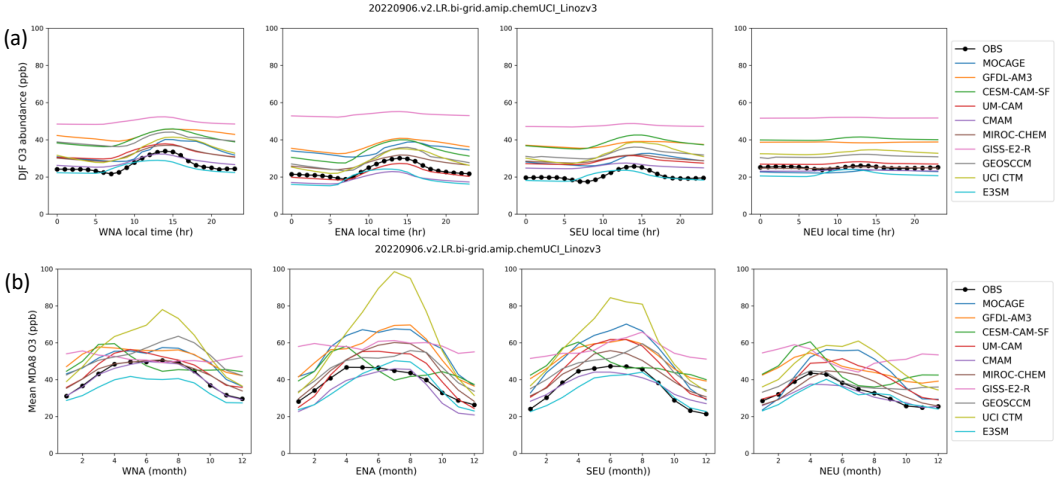

Figure 6. (a) Diurnal cycles of hourly O_3 abundance (units: ppt) for observations (OBS; black lines), 8 ACCMIP models listed on Table 1, UCI CTM (yellow-green lines), and E3SM (cyan lines) averaged over winter (DJF) months in WNA, ENA, SEU, and NEU from left panel to right, respectively. (b) Annual cycles of MDA8 O_3 abundance (units: ppt) for observations (OBS; black lines), 8 ACCMIP models listed on Table 1, UCI CTM (yellow-green lines), and E3SM (cyan lines) in WNA, ENA, SEU, and NEU from left panel to right, respectively.

https://doi.org/10.5194/gmd-2023-203
Preprint. Discussion started: 19 January 2024

Geoscientific Model Development Discussions

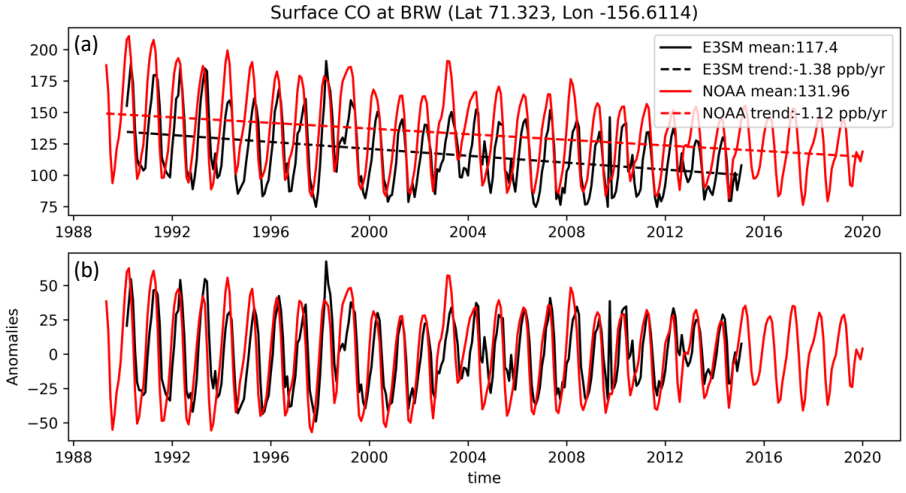

Figure 7. (a) Time series of surface CO burden (units: ppb) from observation (red solid line) and E3SM (black solid line) at the BRW observational site listed on Table 3. Red dotted line and black dotted line show the tendency of surface CO burden of observation and E3SM, respectively. (b) Evolution of anomalies of surface CO burden from observation (red solid line) and E3SM (black solid line).

https://doi.org/10.5194/gmd-2023-203
Preprint. Discussion started: 19 January 2024

Geoscientific Model Development
Discussions
Open Access
EGU

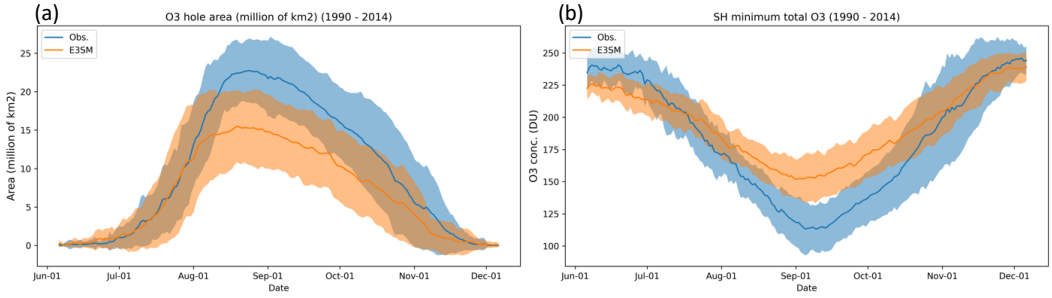

Figure 8. Daily evolution of the Antarctic ozone hole from 1 July to 31 December as measured by (a) area (10^6 km^2) and (b) minimum total column ozone (DU). Results are shown for the model (orange lines) and observations (blue lines) from the NASA ozone watch data for 1990-2019. The shaded area covers ± 1 standard deviation of the multi-year variability for each day.

https://doi.org/10.5194/gmd-2023-203
Preprint. Discussion started: 19 January 2024

Geoscientific Model Development Discussions
Open Access
EGU

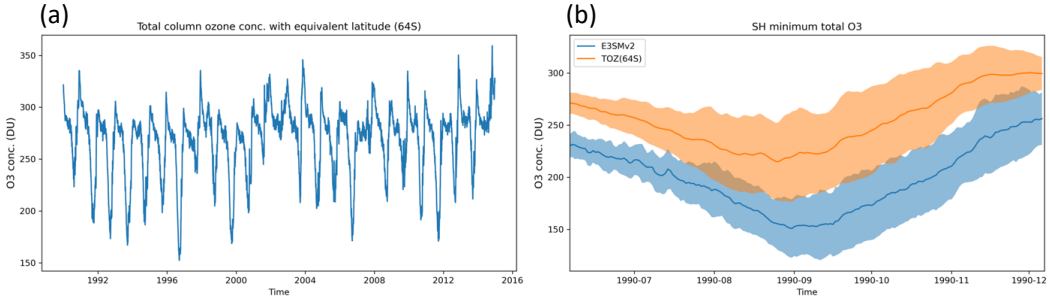

Figure 9. (a) Time series of the minimum total column ozone (DU) with equivalent latitude (64S) area from 1 July to 31 December over the years 1990-2014. (b) Daily evolution of the Antarctic ozone hole from 1 July to 31 December as measured by the minimum total column ozone (DU). Results are shown for the model (blue line) and derived from (a) (orange line). The shaded area covers ± 1 standard deviation of the multi-year variability for each day.

https://doi.org/10.5194/gmd-2023-203
Preprint. Discussion started: 19 January 2024

Geoscientific Model Development Discussions

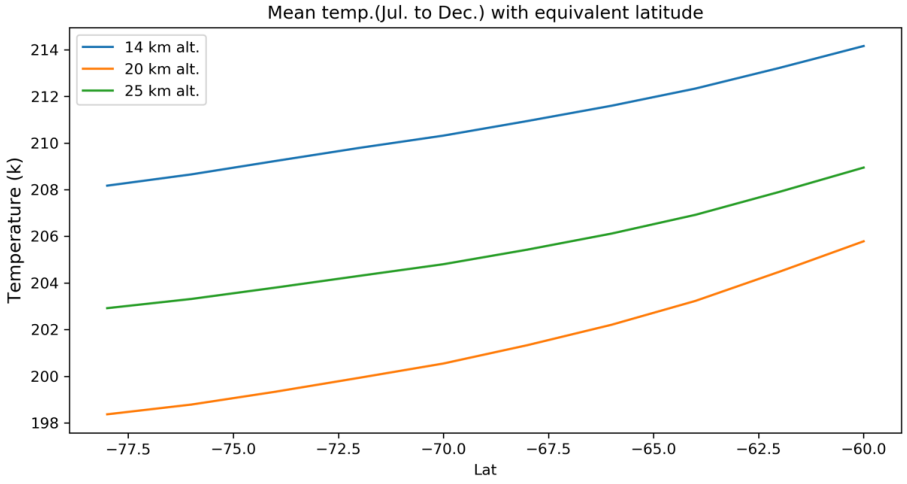

Figure 10. Mean temperature averaged from 1 July to 31 December over the years 1990-1999 at 14, 20 and 25 km altitude with equivalent latitudes from 60°S to 78°S.

https://doi.org/10.5194/gmd-2023-203
Preprint. Discussion started: 19 January 2024

Geoscientific Model Development
Discussions
Open Access
EGU

875

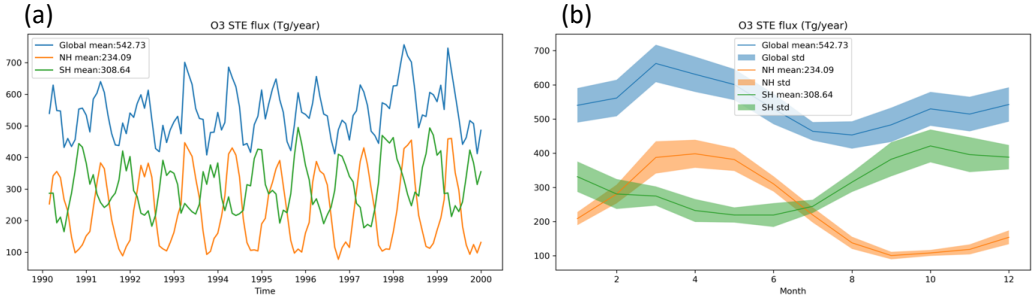

876
877 Figure 11. (a) Time series of the stratosphere troposphere exchange (STE) ozone fluxes (unit:
878 Tg/year) over the years 1990-2000. (b) Mean annual cycle of STE ozone fluxes in the north
879 hemisphere (NH; orange line), south hemisphere (SH; green line) and global (blue line). The
880 shaded area covers ± 1 standard deviation of the multi-year variability for each month.
881
882

https://doi.org/10.5194/gmd-2023-203
Preprint. Discussion started: 19 January 2024

Geoscientific Model Development Discussions
Open Access
EGU

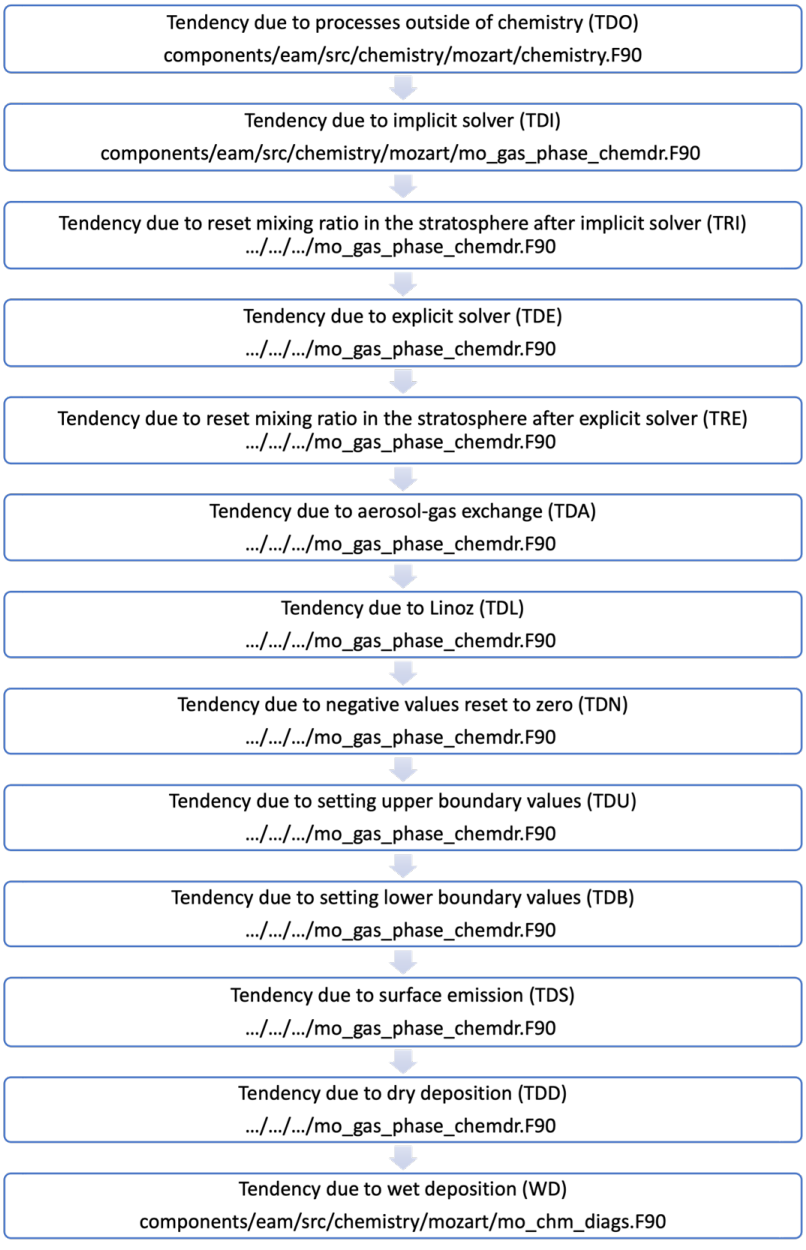

Figure 12. A schematic workflow of chemistry tendency processes and their associated working files.

https://doi.org/10.5194/gmd-2023-203
Preprint. Discussion started: 19 January 2024

Geoscientific Model Development Discussions

888

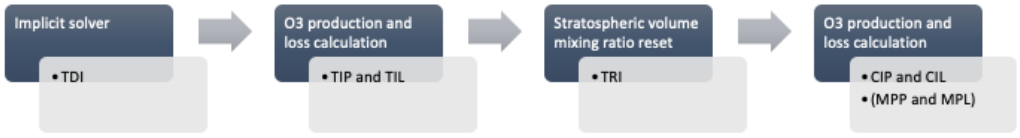

889
890 Figure 13. A schematic workflow of chemistry tendency processes for the ozone production and
891 loss diagnostics in the implicit solver and after stratospheric reset.
892
893